Engineering Analysis with Boundary Elements 135 (2022) 1–11

Contents lists available at ScienceDirect

Engineering Analysis with Boundary Elements

journal homepage: www.elsevier.com/locate/enganabound

Uncertainty quantification and sensitivity analysis of transcranial electric stimulation for 9-subdomain human head model

Anna Šušnjara [a,*], Ožbej Verhnjak [b], Dragan Poljak [a], Mario Cvetković [a], Jure Ravnik [b]

[a] University of Split, Faculty of Electrical Engineering, Mechanical Engineering and Naval Architecture, Split, Croatia
[b] University of Maribor, Faculty of Mechanical Engineering, Maribor, Slovenia

ARTICLE INFO

Keywords:
Analysis of variance
Boundary element method
Stochastic collocation
Transcranial electric stimulation
9-subdomain head model

ABSTRACT

This paper deals with uncertainty quantification of transcranial electric stimulation (TES) of realistic human head model. The head model taken from Visible Human Project consists of 9 subdomains: scalp, skull, CSF, grey matter, white matter, cerebellum, ventricles, jaw and tongue. The deterministic computation of quasi-static induced electric scalar potential features boundary element method (BEM). Conductivities of each subdomain are modelled as uniformly distributed random variables and stochastic analysis features a non-intrusive stochastic collocation method (SCM). The input uncertainties impact only the magnitude of the electric scalar potential and not the position of the potential extrema. Skin and brain conductivities play the most important role, while CSF conductivity has negligible impact on the output potential variance. The significance of the skull conductivity is not high for the chosen input parameter setup. In the previous work authors considered 3-compartment head model which consisted of scalp, skull and brain compartments. The presented model is a step forward in SCM+BEM TES analysis, primarily in terms of model complexity. Comparing the results of the two analyses it can be concluded that the uncertainty in the added tissues' conductivities do not impact the variation of the output electric potential.

1. Introduction

Transcranial electric brain stimulation (TES) is a non-invasive brain stimulation technique used for treatment of various neurological and psychiatric disorders such as depression, anxiety and Parkinson's disease. Electrodes application on the head surface induces the current flow through the head tissues causing the modulation of spontaneous neuronal activity. TES techniques applied according to protocols and procedures are reported to be well tolerated [1]. However, in order to better understand the character of the current distribution in the human head, TES procedures are simulated computationally [2]. The results are then used in the design of TES electrodes and protocols because different electrode positions stimulate different parts of the cortex.

Unfortunately, human head models suffer from uncertainties in the input parameter setup due to several reasons. Generally, uncertainties can be divided into reducible and irreducible ones [3]. The uncertainty which can be reduced by increasing our knowledge, e.g. by performing more experimental investigations and/or developing new physical models is called epistemic or systematic uncertainty. On the other hand, the aleatory or statistical uncertainty cannot be reduced as it rises naturally from the observations of the system. Some additional experiments in this case can only be used to better characterise the variability. When it comes to human head models, both morphology and electric tissue properties (electric permittivity and conductivity) can be sources of uncertainty. Namely, tissue property databases list several values for one parameter of interest. This is because the direct measurements on living humans are not ethically acceptable, hence, reported values originate from various *ex vivo* and in vitro measurements [4,5]. In addition to this, tissue properties vary due to differences in size and shape of each individual's head and general health condition [6,7,8]. The uncertainties originating from limited measurement procedures can be considered as epistemic and those coming from inter-subject variability as aleatory.

One way to alleviate this problem is a stochastic-deterministic approach to TES simulation which requires validated deterministic code and an efficient non-intrusive stochastic method. Intrusive stochastic methods assume the change of formulations and rewriting the solver accordingly, which is a demanding task and very often impossible for anatomically realistic geometries. The non-intrusive stochastic approach is based on post-processing of a number of deterministic

* Corresponding author.
E-mail address: ansusnja@fesb.hr (A. Šušnjara).

https://doi.org/10.1016/j.enganabound.2021.10.026
Received 28 May 2021; Received in revised form 22 October 2021; Accepted 29 October 2021
Available online 22 November 2021

simulations. The stochastic method is efficient if the total number of simulations is relatively low while keeping the precision and accuracy of the estimation of stochastic features for the model output. The stochastic-deterministic analysis of TES is still scarce in the literature. Some examples can be found in the work of Schimdt et al. who investigated the impact of uncertain head tissue conductivity in the optimization of transcranial direct current stimulation for an auditory target [9]. They found that an uncertain conductivity profile can have a substantial influence on the prediction of optimal stimulation protocols for stimulation of the auditory cortex. Likewise, Saturnino et al. investigated the impact of conductivity uncertainty in the computation of electric field in the head tissues for cases of TES and TMS (i.e. transcranial magnetic stimulation) [10]. Contrary to TES, TMS has been widely analysed by means of stochastic-deterministic methods, e.g. in [11,12,13,14,15]. Furthermore, deterministic codes for bioelectromagnetics applications such as TES are mostly based on finite element method (FEM) and such deterministic modelling of various TES scenarios are covered in e.g. [16,17,18,19,20].

This paper should be considered as a follow up of the work published in [21] and [22]. In these two papers a stochastic-deterministic modelling of transcranial electric stimulation featuring the deterministic boundary element method and stochastic collocation method was presented for the first time to the best of the authors' knowledge. While [21] featured a cylindrical representation of human head with geometrical parameters modelled as random variables, the work in [22] was based on anatomically realistic 3-compartment human head model. The conductivities of scalp, skull and brain were modelled as uniformly distributed random variables and the output of interest was distribution of electric scalar potential. The results indicated that the impact of the skull's conductivity is less significant when compared to scalp and skull conductivities for most of the observation points. The deterministic part was compared with FEM based codes used in [9] and [20] showing a good potential of BEM in terms of computational efficiency. Also, the presented stochastic collocation method was comparable to polynomial chaos based approach published in [9]. In this paper the same SCM+BEM stochastic-deterministic approach is used, but with a more complex model geometry, hence the novelty refers to a more complex, 9-subdomain human head model.

The paper is organized as follows. The formulation and human head model are presented in section II along with the short mention of the deterministic boundary element method. Section III outlines the basic principles used for stochastic analysis. Computational results are given in section IV and finally some conclusions regarding the present and the on-going work are given in the final section.

2. Formulation and human head model

Transcranial electric brain stimulation is modelled as a quasi-static electromagnetic problem which means that electric permittivity of biological tissues is neglected [19,23]. Biological tissues in quasi-static approximation are modelled as volume conductors whose inductive component of the impedance is neglected, while resistances, capacitances, and voltage sources are distributed throughout a given 3-dimensional domain [19]. Hence, a human head is modelled as a typical passive volume conductor whose subdomain tissue excitability is ignored. Therefore, the governing equation for the electric scalar potential φ is formulated through Laplace equation [19,22]:

$$\nabla\cdot(-\sigma\nabla\varphi) = 0 \tag{1}$$

where σ is the tissue conductivity.

Dirichlet's type of boundary condition, $\varphi = \pm\varphi_0$, is prescribed at the electrode area and Neumann's type for the rest of the domain, $-\sigma(\partial\varphi/\partial n) = 0$ [22].

The head model depicted in Fig. 1 is a 9-subdomain model of a female head based on a model prepared and published by Noetscher et al.

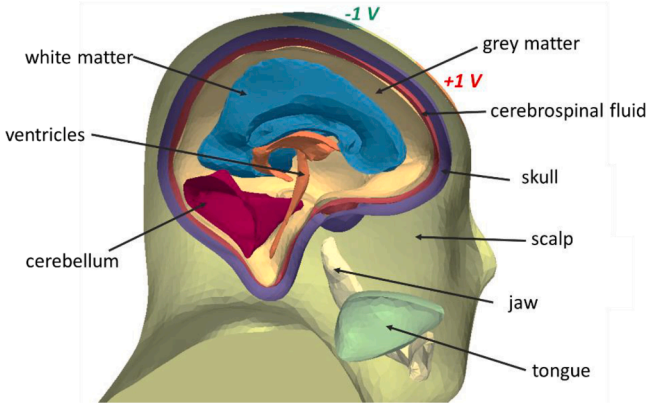

Fig. 1. The 9 subdomains of head model with Cz-Fpz electrode position.

in [16] and Elloian et al. in [17]. The model originates from a Visible Human Project (VHP) of the U.S. National Library of Medicine [24,25]. Also, a detailed description of the model can be found in Makarov et al. [26]. The depicted model consists of 9 tissues: scalp, cerebrospinal fluid (CSF), skull, brain grey matter, white matter part of cerebrum, cerebellum, ventricles, jaw and tongue.

Guidelines for standard electrode position nomenclature define different electrode setups depending on the cortex region that is to be treated [27]. The electrode position chosen in the present work is marked with green and red circles (top of the head and forehead in Fig. 1, respectively). This setup corresponds to Cz-Fpz electrode setup defined by 10/20 electroencephalogram standard for electrode placements [27]; Cz is the central midline electrode and Fpz is the frontopolar midline electrode. The electrodes are of circular shape with the applied potential of $\varphi = \pm 1$ V.

The source for conductivity values is an examination of a large number of studies published in the tissue properties database [28]. The conductivities are modelled as random variables (RV) uniformly distributed in the range defined by their maximal and minimal values reported in [28] (Table 1). Note that ventricles are filled with

Table 1
Conductivity values for 9 subdomains. Maximum and minimum values are reported in [28]. The average value is computed as $\sigma_{avg}=(\sigma_{max}+\sigma_{min})/2$ and coefficient of variation is given as CV (%)$= 100*(\sigma_{max}-\sigma_{avg})/\sigma avg$. The table lists two types of indexes: the Roman numeral denotes the anatomical subdomains in the head while Arabic numeral denotes random variable index (RV index). Maximal RV index is 8 due the same conductivity value for ventricles and CSF. After the OAT analysis the jaw's conductivity is eliminated from stochastic dimensionality which reduces total RV index to 7.

SUBDOMAINS		CONDUCTIVITY VALUES			RV INDEX	
Name	index	$[\sigma_{min}, \sigma_{max}]$ (S/m)	σ_{avg} (S/m)	CV (%)	$i = 1\ldots d; d = 7$ or 8	
cerebellum (white matter part)	I	[0.22, 1.31]	0.765	71.24	1	1
ventricles	II	[1.59, 1.8]	1.695	6.19	2	2
cerebrospinal fluid = CSF	III	[1.59, 1.8]	1.695	6.19	2	2
grey matter = GM	IV	[0.109, 0.481]	0.295	63.05	3	3
jaw	V	[0.00185, 0.00588]	0.003865	52.13	4	(-)
scalp (skin)	VI	[0.09, 0.25]	0.17	47.59	5	4
tongue	VII	[0.02, 0.67]	0.345	94.20	6	5
cerebrum = WM (white mater)	VIII	[0.0644, 1.20]	0.632	89.87	7	6
skull	IX	[0.256, 0.384]	0.32	20	8	7

cerebrospinal fluid, thus the conductivity of both subdomains is treated as one parameter, i.e. the tissues are considered to be one subdomain. Furthermore, since only one study measured the skull conductivity, we considered 20% uniform distribution around the published value.

When input conductivities are prescribed with fixed values (σ_{avg} from Table 1), a deterministic case of eq. (1) is solved. For a non-intrusive stochastic analysis a validated and trust-worthy deterministic numerical method is of a paramount importance. BEM is a rather novel approach for TES modelling. It is successfully applied to TES application in case of cylindrical head representation in [21] and for 3-layered head model in [22], hence, there can be found a more detailed description of BEM for TES application. Also, general mathematical description of BEM numerical approach can be found elsewhere, e.g. in [29].

3. Methods of stochastic analysis

3.1. Computation of stochastic mean and standard deviation

A non-intrusive stochastic collocation method (SCM) is a method of choice for the propagation of uncertainties present in input conductivities to the output electric scalar potential. By following the SCM algorithm published in [30] and [31], the electric scalar potential, φ, obtained by a full model, i.e. eq. (1), can be approximated by its surrogate φ constructed by the following expression:

$$\varphi = \sum_k^n p_k(\sigma)\cdot\varphi_k \tag{2}$$

where φ_k is the value of electric scalar potential from the *k-th* deterministic BEM computation, $k = 1, \ldots n$, $\boldsymbol{\sigma}=[\sigma_1, \sigma_2, \ldots, \sigma_d]$ is a vector of input conductivities modelled as RVs, d is their total number, and $P_k(\boldsymbol{\sigma})$ is *k-th* basis function.

The surrogate from eq. (2) is easily introduced into well-known expressions for stochastic moments thus leading to formulas for the first two stochastic moments of the electric scalar potential [31]: Mean or expectation of the electric scalar potential denoted by $Exp(\varphi)$:

$$Exp(\varphi) \approx \sum_{k=1}^n \varphi_k\cdot\omega_k \tag{3}$$

standard deviation and variance as measures of dispersion denoted by Std(φ) and Var(φ), respectively:

$$[Std(\varphi)]^2 = Var(\varphi) \approx \sum_{k=1}^n \varphi_k^2\cdot\omega_k - [Exp(\varphi)]^2 \tag{4}$$

In eq. (3)-(4) ω_k is the weight of the *k-th*D-dimensional input point computed as $\omega_k = \int_{\Omega}[P_k(\boldsymbol{\sigma})\cdot f(\boldsymbol{\sigma})]d\boldsymbol{\Omega}$; $f(\boldsymbol{\sigma})=\prod_i f(\sigma_i)$ is the joint probability density function, $f(\sigma_i)$ is the *i th* uniform probability density function defined by the data in Table 1; $i = 1, 2, \ldots d$.

Hence, depending on the choice of basis function in eq. (2) and integration rule for computation of the weight ω_k, different variants of stochastic collocation are constructed. In this paper the following choice is made. For one-dimensional stochastic problem, i.e. $\boldsymbol{\sigma}=[\sigma_i]$, $i = 1, 2, \ldots$ *or d*, the basis function is of Lagrange type and the simulation points are chosen according to a Clenshaw-Curtis (CC) or Gauss-Legendre (GL) integration rule for the domain $[\sigma_{i\text{-min}}, \sigma_{i\text{-max}}]$. For D-dimensional stochastic model the sparse grid algorithm is used in order to construct the D-variate basis function preserving the Lagrange basis and CC quadrature rule in each dimension. The reason for CC integration rule in D-dimensional problem is the fact that underlying integration nodes exhibit nested property which reduces the total number of simulations, n with respect to GL quadrature rule. More details can be found in [30].

3.2. Sensitivity analysis

Once the process of computation of mean and variance of electric scalar potential is defined it is possible to carry out the sensitivity analysis (SA) based on the variance computation. The aim is to investigate to which extent the variability of each input conductivity impacts the dispersion of the output potential around its expected value.

The first approach to carry out SA is to simply compare variances of all 1-dimensional cases, a so called "one-at-a-time" (OAT) approach [31]. The higher the variance of *i th* 1-dimensional case the bigger the impact of the *i th* conductivity.

However, OAT approach cannot detect if interactions amongst the variables have some significant impact on the output. Based on Hoeffding decomposition of total variance in D-dimensional stochsastic case, Sobol defined a set of indices that cover all possible input parameter interactions and their impact on the output value [32]. The first order Sobol index gives the information about the impact each input variable has on the output [33]:

$$S1_i = \frac{Var_{\sigma_{\sim i}}\left[Exp_{\sigma_{\sim i}}(\varphi|\sigma_i)\right]}{Var[\varphi|\sigma_1, \sigma_2, \ldots\sigma_n]} \tag{5}$$

S1 here denotes the first order index, while the integer i in the subscript denotes the input parameter, i.e. $S1_3$ is the 1st order index for the σ_3. The tilde "∼" sign in the equations means "all ecxept", and the vertical line "|" denotes the conditional expectation and conditional variance.

Higher order Sobol indices (*S2, S3, …, S7*) give information about the impact of interactions amongst the parameters, e.g. $S2_{12}$ is the second order sensitivity index (*S2*) that gives information about the interaction between the first two parameters (1 and 2 in the subscript, i.e. σ_1 and σ_2 – the interaction between the cerebellum and white matter conductivities).

However, computation of higher order sensitivity indices may be time consuming, hence a total effect index is computed instead. Total effect index gives the information about the impact each input parameter has on the output along with its own interaction with other parameters considering all possible combinations. The formula is as follows [33]:

$$ST_i = 1 - \frac{A_{ar_{\sigma_{\sim i}}}\left[Wxp_{\sigma_{\sim i}}(\varphi|\sigma_{\sim i})\right]}{Var[(\sigma_1, \sigma_2, \ldots\sigma_n)]} \tag{6}$$

If *S1* and *ST* indices for *i th* parameter are of the same value then, the *i th* parameter interaction with other parameters is negligible. Parameters whose *ST* is very small can be completely neglected as RVs and should be modelled as fixed/deterministic values instead. Also, parameters whose OAT impact is very small can be eliminated as RVs.

Note that conditional variances and expectations in eq. (5)-(6) are computed by means of stochastic collocation method. The described approach is popularly called the ANalysis Of VAriance approach in the literature (ANOVA) [33].

4. Computational results

4.1. Computational mesh analysis

In order to establish that the computational grid of the presented 9-layer head model does not influence the results, electric potential is simulated on different grids each time using the same conductivity parameter settings (the average conductivity values). Triangular elements are used and the resulting meshes count between 36 and 87 thousand degrees of freedom (nodes and centres of elements). Potential profiles obtained using different meshes are compared in Fig. 2 and small differences can be observed between them. In order to save computational time, the subsequent calculations are performed with 45 thousand degrees of freedom mesh.

4.2. Convergence of stochastic collocation method

The analysis starts with 8-dimensional stochastic problem since ventricles and CSF are treated as one subdomain in terms of electric

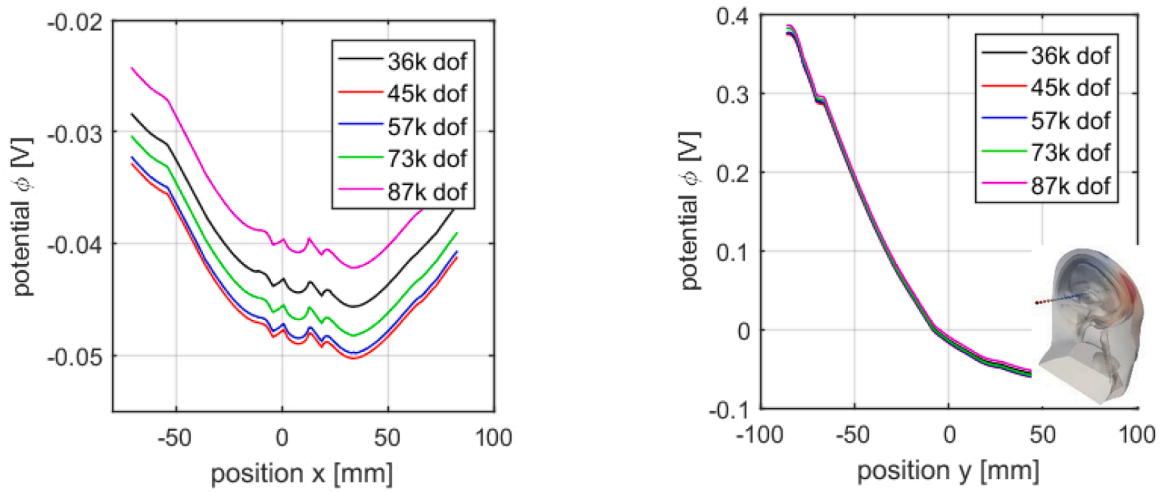

Fig. 2. Comparison of potential profiles left-to-right (left panel) and front-to-back (right panel) obtained using different computational meshes. Only small differences between meshes are observed. Due to high conductivity of cerebrospinal fluid, we observe constant potential in this region.

conductivity value. Stochastic computations are carried out firstly according to OAT approach, i.e. keeping 7 conductivities at fixed value and modelling only one of them as RV at a time. The indexing of the "stochastic" subdomains in this case corresponds to $i = 1, 2, \ldots 8$ as denoted in Table 1.

Gauss-Legendre (GL) quadrature is used for computation of stochastic moments in OAT analysis. The convergence is tested by changing the number of collocation points (CP), i.e. deterministic simulations ($n = 3, 5, 7$ & 9). Different n sizes are also called the Design of Experiment or DoE. The potential expectation and standard deviation are depicted in Fig. 3 for different n sizes in case when the only RV is CSF conductivity, i.e. $i = 2$. The convergence for both expectation and standard deviation is satisfactory.

Furthermore, the error function (E_r) and Euclidean norm are computed according to the following expressions:

$$E_r = \| A_j^{i+1} - A_j^i \| \Big/ \| A_j^i \|, \; i = 1.2, \ldots N-1$$
$$\| A_j^i \| = \sqrt{\sum_{J=1}^{J} \left| A_j^i \right|^2} \tag{7}$$

where A corresponds to either $Exp(\varphi)$ or $Std(\varphi)$ at j-th observation point of interest. N stands for total number of different DoEs used for stochastic analysis (different n sizes). For example, in OAT analysis there are four DoEs, i.e. $n = 3, n = 5, n = 7, n = 9,$ therefore $N = 4$.

The results for E_r in OAT analysis are depicted in Fig. 4. It can be

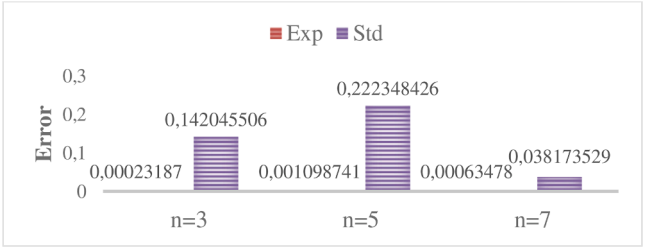

Fig. 4. The convergence for expectation and standard deviation of electric potential computed according to eq. (7). n is total number of simulations, Exp is potential expectation and Std is potential standard deviation.

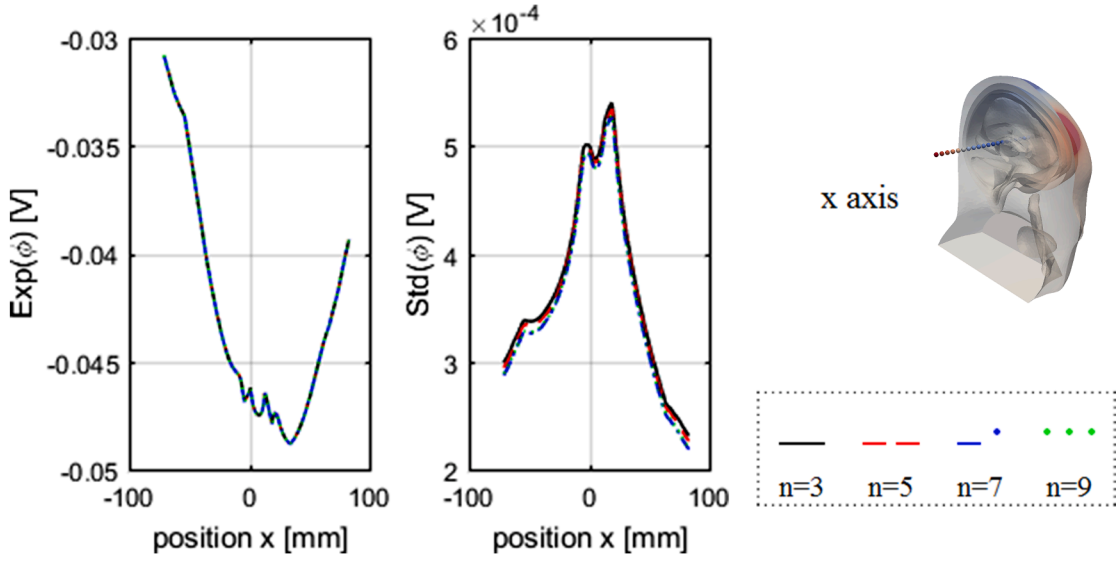

Fig. 3. The influence of the total number of deterministic simulations (n) on results of OAT analysis. The RV is the cerebrospinal fluid's conductivity ($i = 2$). The panels show potential expectation (left) and potential standard deviation (right) along the chosen x axis. The number of collocation points (n) has larger influence on higher order moment, i.e. standard deviation.

observed that the error for potential expectation is negligible for all DoEs, while the error for standard deviation decreases to value of 0.0381.

Since the variance of jaw conductivity is very small (depicted in Fig 5 in the later section), the number of subdomains for the D-dimensional stochastic problem is reduced from $d = 8$ to $d = 7$. The 7-dimensional stochastic problem is treated by means of a sparse grid SC. The maximal total number of simulation points is 589 which corresponds to a 9CP Clenshaw-Curtis (CC) integration rule in each dimension. The 3CP and 5CP CC quadrature in each dimension result in 15 and 113 total number of simulations, respectively. Hence, the convergence of the stochastic collocation method is tested by comparing the 15, 113 and 589 designs of experiment (DoEs) and results are depicted in Fig. 5. The expectation and standard deviation curves for sample sizes $n = 113$ and $n = 589$ are close to each other, while $n = 15$ has poor convergence. The Fig. 5 indicates that DoE with 113 simulations can be used for stochastic analysis. The results in Fig. 5 are depicted for two axes in head model: front-to-back and left-to-right, however the conclusions are valid for all points of observation.

The E_r results for potential expectation and standard deviation along the x and y axis in case of 7-dimensional stochastic model are depicted in Fig. 6. It can be observed that the error decreases to values below 0 for both expectation and standard deviation.

4.3. OAT analysis

Once the convergence of the proposed stochastic-deterministic approach is confirmed to be satisfactory the stochastic analysis of the output electric scalar potential can be carried out. The results for the standard deviations of 8 one-dimensional cases are depicted in Fig. 7 for observation points along x and y axis, where x axis is orientated across the head (left-to-right) while the y axis is orientated along the head model (front-to-back). Examining the distributions of 8 standard deviations it is clear that the jaw conductivity has a negligible impact while scalp, grey matter and white matter conductivities have the highest impact.

Fig. 8 shows average conductivity values and their respective coefficients of variation given in Table 1 compared to the maximal potential variance for every head subdomain after OAT stochastic analysis of individual tissues. The negligible impact of jaw conductivity is obvious, once again. Although the jaw conductivity varies 52.13% around its average, evidently its expected value is too small in order to significantly impact the variability of the output scalar potential. Therefore, it is excluded from the stochastic dimensionality and the following results are obtained for a 7-dimensional stochastic model as shown in Table 1. The highest influence pertains to scalp and brain tissue conductivities (white and grey matter). CSF conductivity is very high, yet its influence is not as important as expected which could be due to its low coefficient of variation (CV). This result is in accordance to findings in [9] and [10]. The similar conclusion can be stated for tongue conductivity; its impact does not follow its very high CV of 94.2%.

4.4. Confidence intervals and stochastic moments

Confidence interval (CI) of $\pm 3 \cdot Std(\varphi)$ is chosen in order to represent the spread of the possible potential values with a confidence level of 99%. Hence, confidence intervals computed as $CI = Exp(\varphi) \pm 3 \cdot Std(\varphi)$ are depicted in Fig. 9 for two different profiles (observation points are along x and y axis, respectively). The width of CI is rather evenly distributed along x axis which is orientated from the left to the right side of the head. On the other hand, the width of the CI along y axis which is orientated front-to-back tends to decrease since CI is the widest around the electrode area.

Distributions of mean and standard deviation of electric scalar potential on the surface of head model subdomains are depicted in Figs. 10 and 11. The standard deviation distribution follows the trend of the expected electric scalar potential, i.e. the points with maximal absolute value of expected potential have the highest variance, and therefore the highest standard deviation. This is important finding; the character of the potential distribution remains the same, i.e. the points of maximal or minimum potential won't change the position to some greater extent due to the uncertain input parameter. The uncertainties impact only the magnitude of the electric scalar potential at certain observation point of interest. This is in accordance with results reported in [10].

The highest standard deviation is observed in the close area around the electrodes. Also, when observation points move from one subdomain to another, again the largest deviation is observed under the electrodes. The maximal dispersion of the potential, i.e. standard deviation, is of

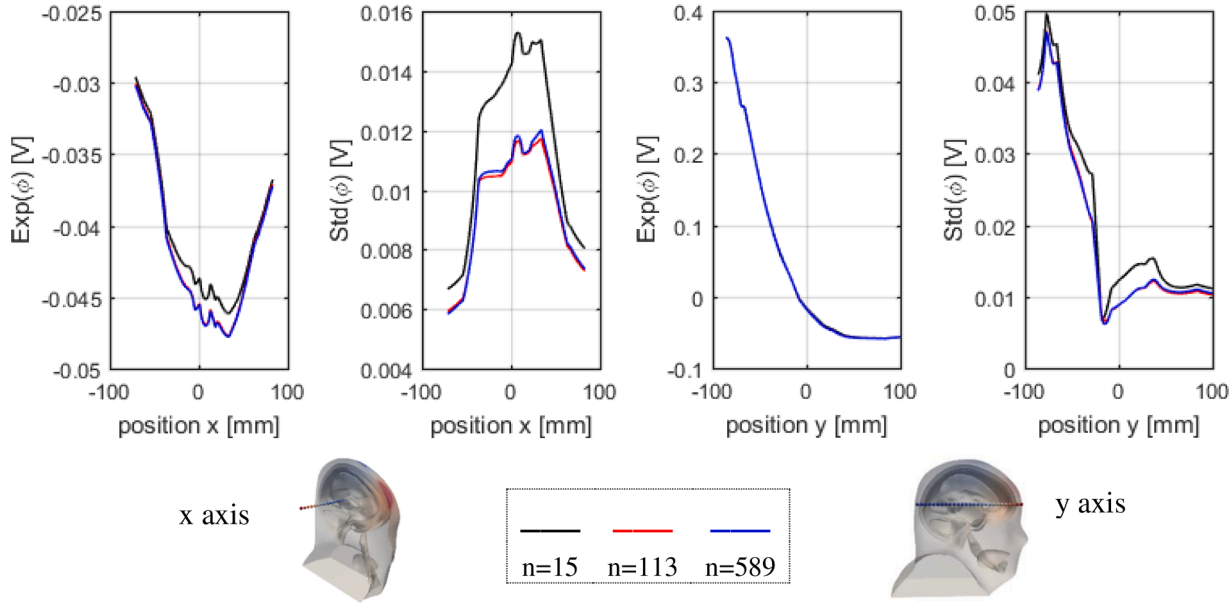

Fig. 5. The influence of the number of deterministic simulations $n = 15, 113, 589$, for the 7-dimensional stochastic model. The panels show potential expectation and potential standard deviation along the x axis (left) and y axis (right). The number of collocation points has larger influence on the higher order moment, i.e. standard deviation.

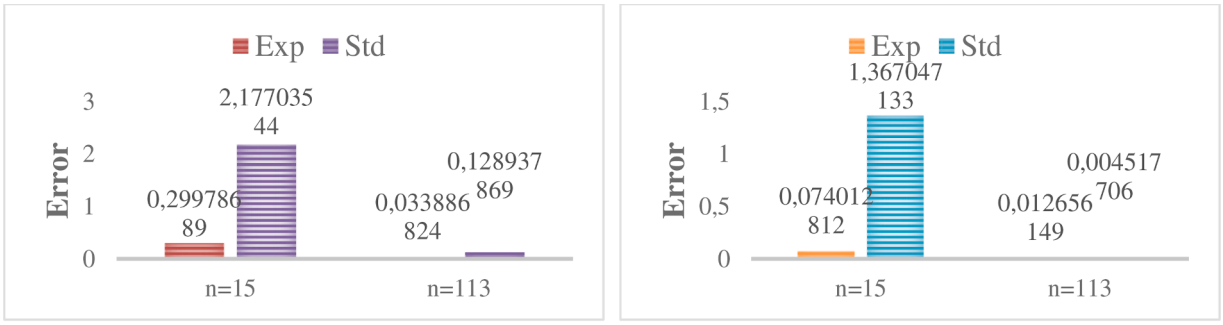

a) x axis b) y axis

Fig. 6. The convergence for expectation and standard deviation of electric potential computed according to eq. (7) for observation points along the a) x axis and b) y axis. n is total number of simulations, Exp is potential expectation and Std is potential standard deviation.

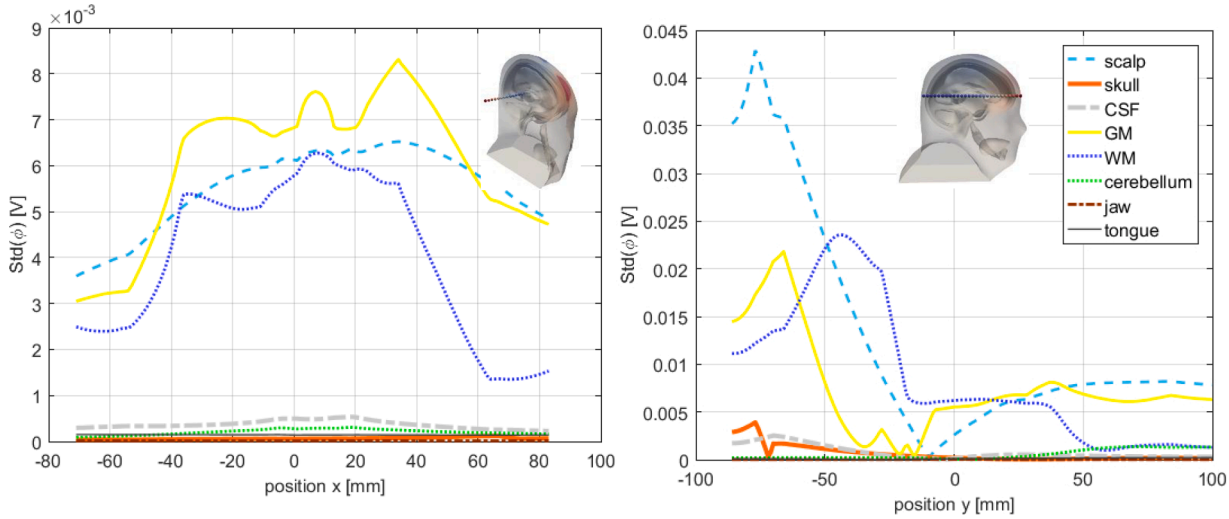

Fig. 7. Comparison of electric potential standard deviation for left-to-right (left panel) and front-to-back (right panel) profiles obtained using OAT study of different tissue conductivities. Five control points are used.

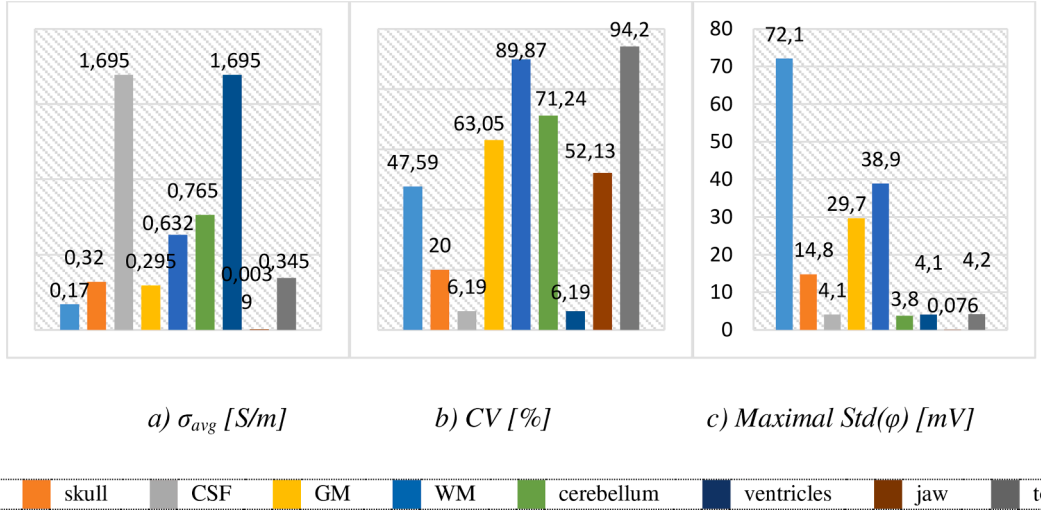

Fig. 8. Comparison of: average conductivity values (a), coefficient of variation (b) and maximal electric potential standard deviation found using the OAT stochastic analysis of individual tissues (c). Five collocation points were used for the latter. Note that ventricles and CSF are the same region.

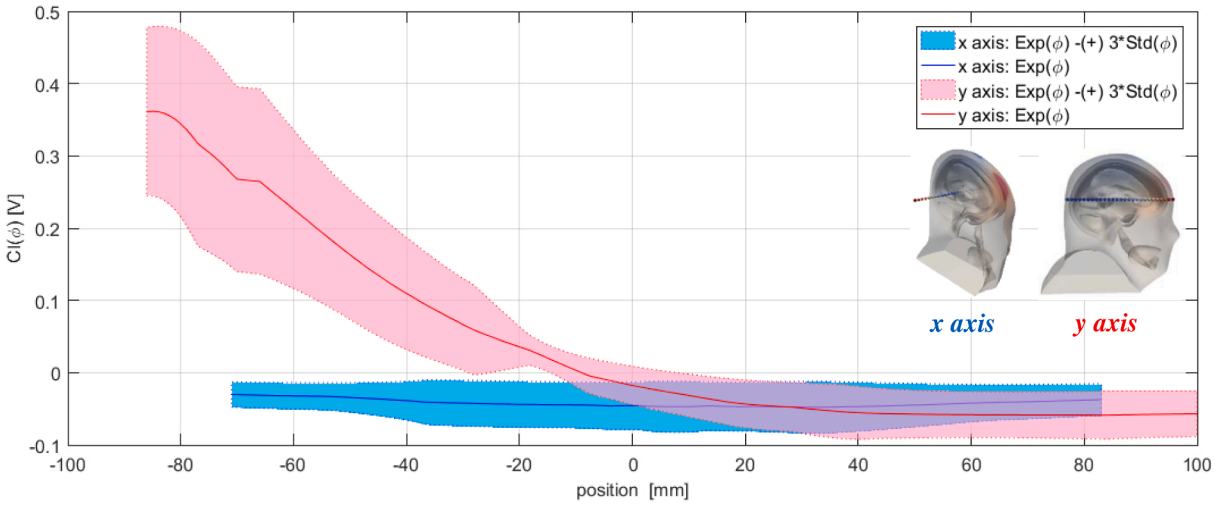

Fig. 9. The confidence interval distribution along x and y profiles in the human head. Confidence interval is computed as CI= Exp(φ) ± 3•Std(φ).

order ~50 mV in scalp, skull, CSF and brain (brain representing the white matter part of cerebrum and grey matter) while in cerebellum, ventricles, jaw and tongue it is of order ~10 mV (subdomains in Fig. 10 vs. Fig. 11). The range of values for expected electric potential and potential standard deviation is larger for the 5 subdomains depicted in Fig. 10 compared to 4 regions in Fig. 11.

The results from Figs. 10 and 11 are summarized in Fig. 12 and compared to the input conductivities. When comparing the CSF and ventricles, their conductivities are represented by the same RV but maximal standard deviation is much lower in the ventricles area which is due to their physical position with respect to the electrodes placement. When moving from scalp to inner domains the mean potential decreases, but standard deviation is larger in the first 4 subdomains. Moreover, the largest value of standard deviation is observed in the skull.

4.5. ANOVA sensitivity analysis

The first order sensitivity index (*S1*) is depicted in Fig. 13 for *x* and *y* profiles. Note that more control points, i.e. deterministic simulations could be needed for more accurate computation of *S1* index. Namely, in eq. (5) and (6) conditional expectations and variances are computed several times in order to obtain *S1* which could lead to the propagation of the numerical error present in the computation of expectation and variance values in the first step. Nevertheless, in order to use the maximum of 589 computations for the same analysis, one can observe the trend of *S1* and relative relation of *S1* between the conductivities of 7 subdomains. Thus, it can be concluded that scalp, grey matter and cerebrum (white matter) have more significant impact on the output variance of electric scalar potential compared to other input parameters. When observing all other points of computation, which is omitted here, the conclusion is the same. This is in accordance with results reported in [22]. Note that the impact of the skull conductivity is denoted as "important" in [9] and [10] while here the skull conductivity is amongst the parameters with small impact. The possible reason for this rather different conclusions lies in different approaches to modelling the skull conductivity. Namely, the average value of σ_{skull} in this paper is higher by the order of magnitude compared to skull conductivity in [9] and [10] because here the property database from [28] is used as source of low frequency conductivity values in human body tissues. Note that, since only one reference for skull conductivity is reported in [28] the coefficient of variation CV = 20% is chosen. On the other hand in [9] and [10] the skull's conductivity varies up to 90.8% and 60%, respectively.

5. Discussion

This paper introduces the stochastic-deterministic modelling of a transcranial electric stimulation for 9-subdomain human head model. The presented work is a follow up of stochastic-deterministic modelling of a TES in case of 3-layer head model reported in [22]. In both cases an efficient combination of stochastic collocation and "in-house" boundary element method (SCM+BEM) is used for computation of stochastic moments for electric scalar potential in the human head and for sensitivity analysis of the uncertain input conductivities. Compared to [22], where conductivities of skin, skull and brain were modelled as uniformly distributed random variables (RVs), the present work features the inclusion of other tissues, thus, the total of 9 subdomains are as follows: scalp (skin), skull, cerebrospinal fluid (CSF), grey matter, white matter, cerebellum, ventricles, jaw and tongue. The stochastic collocation enables a non-intrusive approach to stochastic analysis, thus keeping the deterministic formulation unchanged. Furthermore, the boundary element method provides the exact geometrical description of the problem boundary by using the isoparametric transformations. Additionally, it is easier to produce 2D surface meshes of complex domains, such as the human brain, as compared to volume meshes required by e.g. FEM. The drawbacks and the strengths of the presented approach have been documented in [22].

The presented deterministic BEM for 9-layer human head showed good convergence and 45 thousand degrees of freedom mesh is chosen for further stochastic analysis. The stochastic method exhibits a satisfactory convergence for the computation of expectation and standard deviation: a total of 113 deterministic simulations is considered as enough. The method's performance is comparable to stochastic-deterministic approaches reported in [9] and [10] where general Polynomial Chaos (gPCE) and finite element method (FEM) were used.

Namely, Schmidt et al. in [9] considered a 4-layer head model with skull, skin, grey matter and white matter conductivities modelled as uniformly distributed RVs; the average conductivities were 1.6, 280, 220 & 90 mS/m, while relative deviations were 90.8%, 51.3%, 50.6% and 52.6%. Their mesh resulted in 2.2 million degrees of freedom (dof) with residual error of 10^{-7} while gPCE required 465 deterministic simulations, each simulation executed in 80 min.

On the other hand, Saturnino et al. in [10] dealt with 6-layer head model with white matter, grey matter, cerebrospinal fluid, spongy bone, compact bone and scalp modelled as beta distributed RVs with their respective [min-max] as follows: [0.1–0.4] S/m, [0.1–0.6] S/m, [1.2–1.8] S/m, [0.015–0.040] S/m, [0.003–0.012] S/m and [0.2–0.5] S/m. Their model resulted in 4.1 million tetrahedra and 720 thousands of vertices. They reported that the gPCE method converged after 292

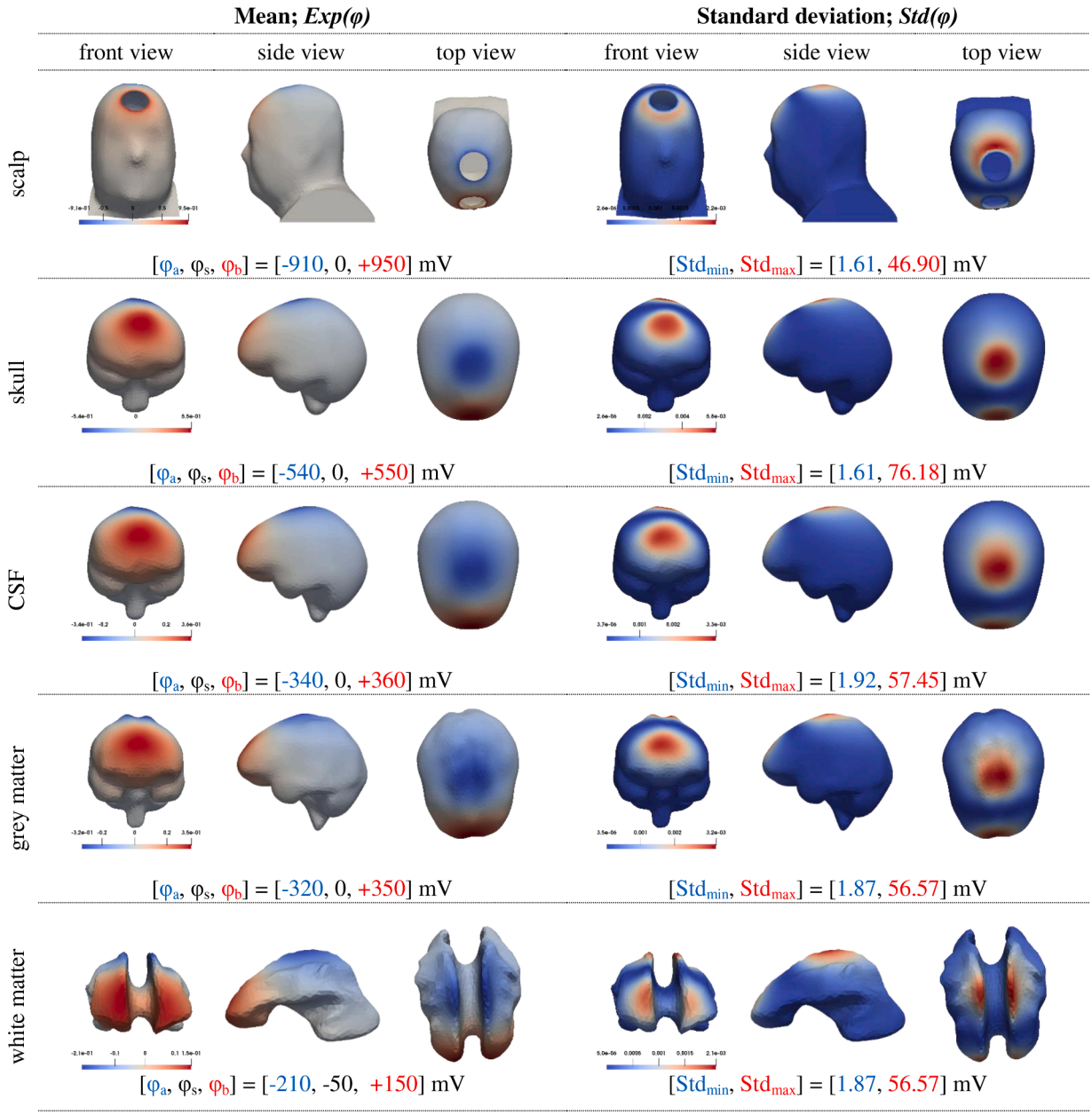

Fig. 10. Distribution of electric scalar potential mean and standard deviation on the surface of head subdomains (part 1). φ_a and φ_b stand for maximal negative and positive potential value, φ_s is minimal absolute potential value.

and 176 FEM simulations for focal tDCS and standard tDCS, respectively (tDCS stands for transcranial direct current stimulation).

Note that, the present paper and [9–10] differ in the electrode setup as well as in the output value of interest; in [9] the induced current density and the anode/cathode currents are observed, while in [10] the distribution of the electric field is the output of interest. Nevertheless, the conclusions about the sensitivity analysis in the papers can be compared.

The stochastic analysis of 9-subdomain TES shows that the points of potential extrema do not change their position due to the uncertain input parameter. The input uncertainties impact only the magnitude of the electric scalar potential which is in accordance with [10]. One-at-a-time (OAT) sensitivity analysis showed that jaw's conductivity has a completely negligible impact on potential variance and standard deviation. It is interesting to note that many input parameters with very high coefficient of variation have small impact on the output potential variation. Furthermore, the CSF conductivity, even though very high, does not impact to greater extent the output potential which is also stated in [10], while in [9] the CSF is treated as a known input parameter, i.e. deterministic parameter. Nevertheless, the region of the CSF subdomain shows rather high values of potential expected value and variance/ standard deviation because of its high average conductivity. Note that CSF is a so called "super highway" for current flow, according to Bikson et al. [34].

Furthermore, the findings from [22] are confirmed: scalp, grey matter and cerebrum (white matter) have more significant impact on the output variance of electric scalar potential w.r.t to other input parameters. This is also in accordance with results reported in [9] and [10].

However, while conclusions about the distribution of the expected potential and variance/ standard deviation, as well as scalp and brain impact are the same as in [9–10], there is a significant difference in the conclusions regarding the impact of the skull conductivity. Namely, in the present paper and in [22] the impact of the skull's conductivity is classified as not important when compared to skin and bran

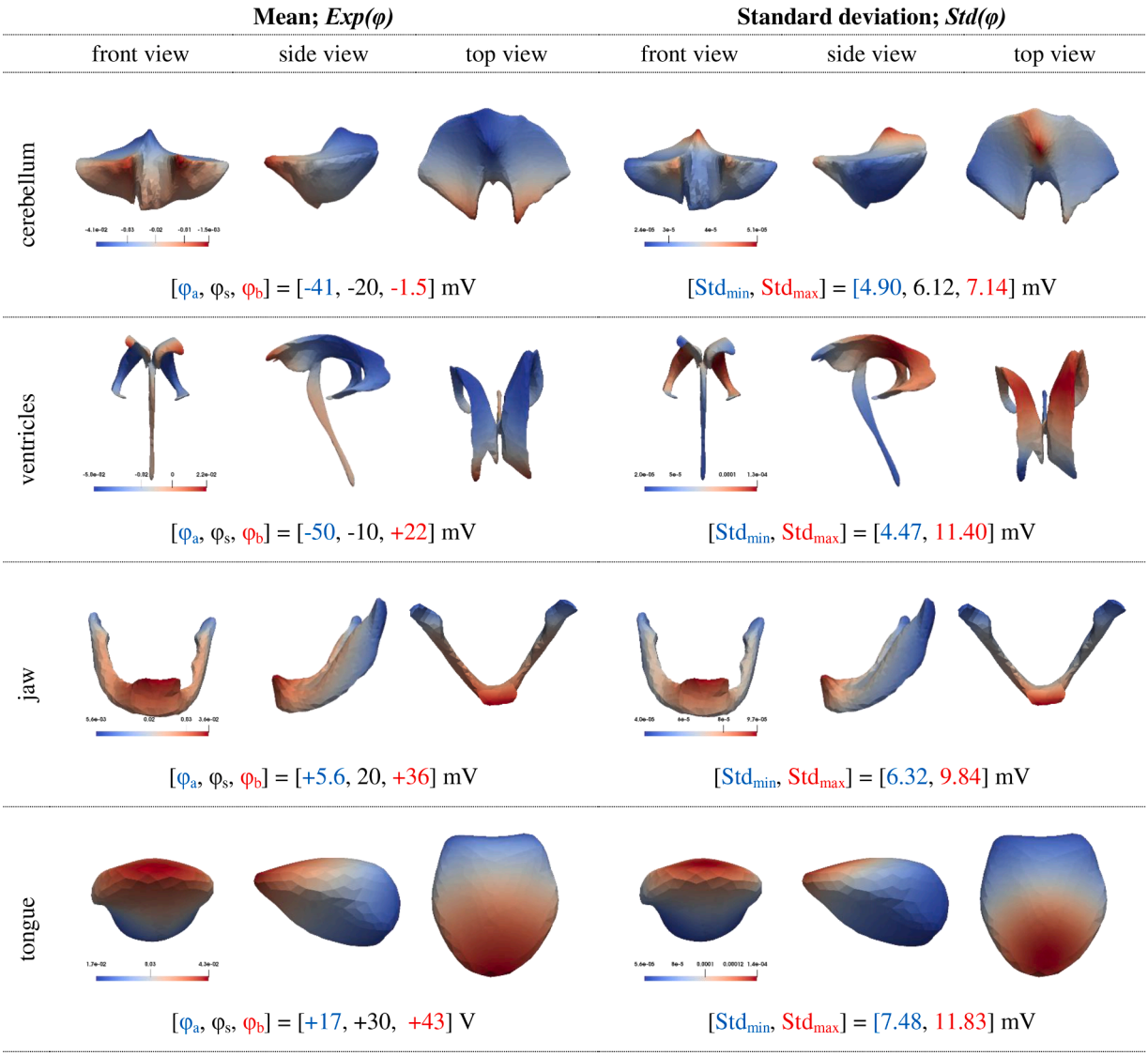

Fig. 11. Distribution of electric scalar potential mean and standard deviation on the surface of head subdomains (part 2). φ_a and φ_b stand for maximal negative and positive potential value, φ_s is minimal absolute potential value.

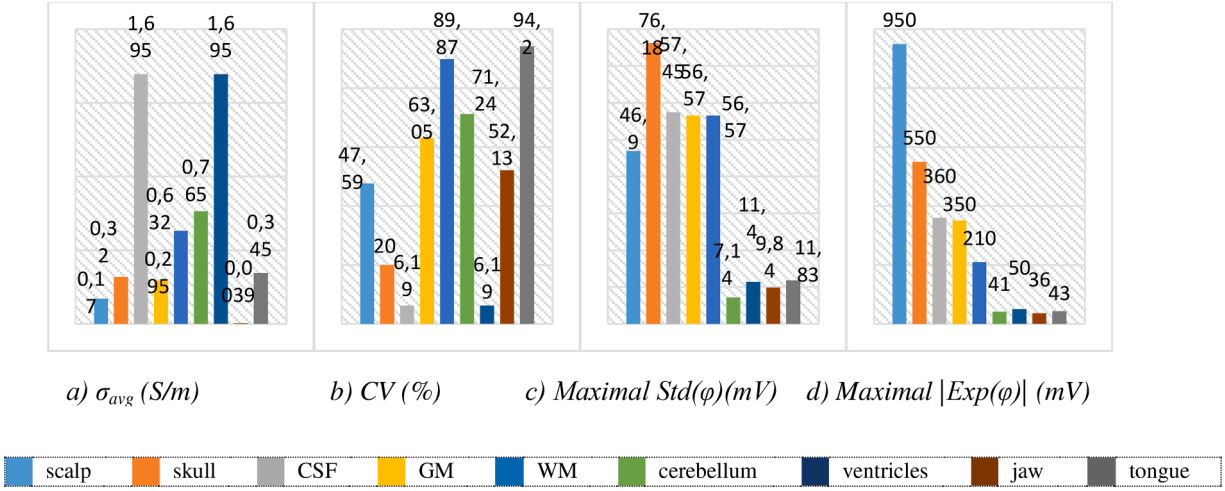

Fig. 12. Comparison of: average conductivity values (a), coefficient of variation (b), maximal standard deviation of electric scalar potential in each domain (c) and maximal expected potential for each subdomain (d). The results depicted in (c) and (d) are for 7-dimensional stochastic model.

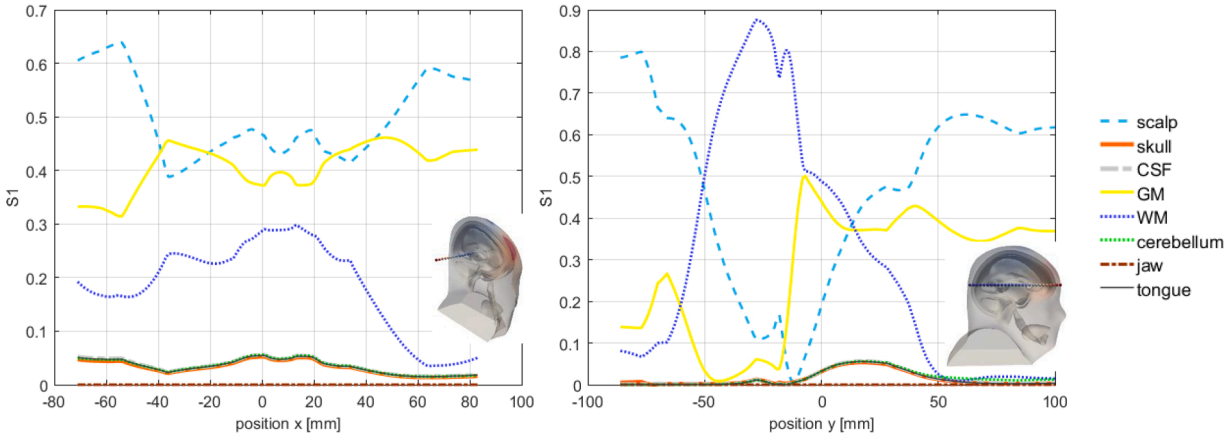

Fig. 13. The first order sensitivity index for observation points along the axis x and y, left-to-right and front-to-back axis, respectively.

conductivities. However, in [9] and [10] skull's conductivity plays an important role. The reason for this disagreement lies in different approaches to modelling the skull conductivity; here, both the conductivity's average and coefficient of variation are much lower.

Finally, in this work a simplified example of ±1 V electrode setup is considered and the output value of interest is electric scalar potential. In addition, the source of conductivity values is property database from [28] which is not the case for other reported stochastic analyses such as [9–10] which refer to different conductivity sources. Therefore, future work shall be orientated towards the investigations of different uncertainty quantifications of skull conductivity and electrode setups.

6. Conclusion

Stochastic-deterministic modelling of TES for 9-subdomain human head featuring the stochastic collocation and boundary element method (SCM+BEM) has been undertaken in this paper. The conductivities of scalp (skin), skull, cerebrospinal fluid (CSF), grey matter, white matter, cerebellum, ventricles, jaw and tongue are modelled as uniformly distributed random variables and stochastic moments of the output electric scalar potential are computed. Also, sensitivity analysis is carried out in order to rank input conductivities with respect to the influence their uncertainty has on variation of the electric scalar potential values.

Uncertainty quantification of the output electric scalar potential shows that the input uncertainties impact only the potential magnitude, i.e. the points of potential extrema do not change their position due to the uncertain input parameter. For this reason, the higher standard deviation has been computed in the area below the electrodes. Sensitivity analysis shows that scalp and brain (grey matter and white matter) conductivities have the most significant impact on variation of the electric potential values. In the previous work authors considered 3-compartment head model which consisted of scalp, skull and brain compartments. Therefore, the presented model is a step forward in SCM+BEM TES analysis, primarily in terms of model complexity. More subdomains require additional stochastic dimensions which increases overall complexity of the approach. Nonetheless, the SCM+BEM procedures have shown a satisfactory convergence.

Furthermore, comparing the results of the two analyses (3-compartment an 9-subdomain models) it can be concluded that the impact of the added parameters, i.e. conductivities of the cerebrospinal fluid (CSF), cerebellum, ventricles, jaw and tongue can be neglected. This means that the stochastic dimensionality can be reduced to total of 3 even for the 9-subdomain head model.

The presented results are comparable to results obtained by different stochastic-deterministic approaches reported in the literature. Some strengths of the SCM+BEM method compared to other approaches have been discussed; while SCM allows relatively small number of deterministic solutions, the BEM provides the exact geometrical description of the problem boundary through the isoparametric transformation.

In the future work other electrode setups shall be considered and more realistic TES examples will be covered. Also, the comparison between different sources of conductivity values for head tissues will be carried out.

Declaration of Competing Interest

The authors declare no conflict of interest.

Acknowledgement

This work was supported by the Croatian Ministry of science, education and sports and Slovenian Research Agency (research core funding No. P2–0196 and bilateral agreement BI-HR/18–19–010).

References

[1] Antal A. "Low intensity transcranial electric stimulation: safety, ethical, legal regulatory and application guidelines". Clin Neurophysiol 2017;128(9):1774–809.
[2] Rush S, Driscoll DA. "Current distribution in the brain from surface electrodes". Anesth Analg 1968;47(6):717–23.
[3] Iaccarino G. Uncertainty quantification in simulations of reactive flows. Marseille; 2012.
[4] C. Gabriel, "Compilation of the dielectric properties of body tissues at RF and microwave frequencies", Technical Report: AL/OE-TR-1996-0037, TX: Brooks Air Force Base; 1, 1996..
[5] Gabriel C, Peyman A. "Dielectric measurement: error analysis and assessment of uncertainty". Phys Med Biol 2006;51(23).
[6] Bikson M, Rahman A, Datta A, Fregni F, Merabet L. "High-resolution modeling assisted design of customized and individualized transcranial direct current stimulation protocols". Neuromodulation 2012;15:306–15.
[7] Parazzini M, Fiocchi S, Cancelli A, Cottone C, Liorni I, Ravazzani P, Tecchio F. "A Computational Model of the Electric Field Distribution due to Regional Personalized or Nonpersonalized Electrodes to Select Transcranial Electric Stimulation Target". IEEE Trans Biomed Eng 2017;64(1):184–95.
[8] Laakso I, Tanaka S, Koyama S, Santis VD, Hirata A. "Inter-subject variability in electric fields of motor cortical tDCS". Brain Stimul 2015;8(5):906–13.
[9] Schmidt C, Wagner S, Burger M, Rienen U, Carsten HW. "Impact of uncertain head tissue conductivity in the optimization of transcranial direct current stimulation for an auditory target". J Neural Eng 2015;12(4):1–12.
[10] Saturnino GB, Thielscher A, Madsen KH, Knösche TR, Weise K. "A principled approach to conductivity uncertainty analysis in electric field calculations". Neuroimage 2019;188:821–34.
[11] Codecasa L, Di Rienzo L, Weise K, Gross S, Haueisen J. "Fast MOR-Based Approach to Uncertainty Quantification in Transcranial Magnetic Stimulation". IEEE Trans Magn 2016;52(3).
[12] L. Codecasa, L. Di Rienzo, K. Weise and J. Hausien, "Uncertainty quantification in transcranial magnetic stimulation with correlation between tissue conductivities", in International Applied Computational Electromagnetics Society Symposium (ACES), Florence, Italy, 2017.
[13] Weise K, Di Rienzo L, Brauer H, Haueisen J, Toepfer H. "Uncertainty Analysis in Transcranial Magnetic Stimulation Using Nonintrusive Polynomial Chaos Expansion". IEEE Trans Magn 2015;51(7).

[14] C. Li and T. Wu, "Impact of uncertain transcranial magnetic stimulation coil position and orientation in the stimulation for a motor cortex", in XXXIInd General Assembly and Scientific Symposium of the International Union of Radio Science (URSI GASS), Montreal, QC, Canada, 2017.
[15] M. Cvetkovic, A. Susnjara, D. Poljak, S. Lallechere and K. El Khamlichi Drissi, "Stochastic Collocation Method Applied to Transcranial Magnetic Stimulation Analysis", in he Joint Annual Meeting of The Bioelectromagnetics Society and the European BioElectromagnetics Association, BIOEM 2016, Ghent, Belgium, 2016.
[16] Noetscher GM, Yanamadala J, Makarov SN, Pascual-Leone A. "Comparison of cephalic and extracephalic montages for transcranial direct current stimulation–a numerical study". IEEE Trans Biomed Eng 2014;61(9):2488–98.
[17] Elloian JM, Noetscher GM, Makarov SN, Pascual-Leone A. "Continuous wave simulations on the propagation of electromagnetic fields through the human head". IEEE Trans Biomed Eng 2014;61(6):1676–83.
[18] Laakso I, Hirata A. "Computational analysis shows why transcranial alternating current stimulation induces retinal phosphenes". J Neural Eng 2013;10(4).
[19] Bai S, Loo C, Dokos S. "A review of computational models of transcranial electrical stimulation". Crit Rev Biomed Eng 2013;41(1):21–35.
[20] Lee C, Kim E, Im CK. "Techniques for Efficient Computation of Electric Fields Generated by Transcranial Direct-Current Stimulation". IEEE Trans Magn 2018;54 (5):1–5.
[21] A. Šušnjara, J. Ravnik, O. Verhnjak, D. Poljak and M. Cvetković, "Stochastic-Deterministic Boundary Integral Method for Transcranial Electric Stimulation: a Cylindrical Head Representation", in 27th International Conference on Software, Telecommunications and Computer Networks, SoftCOM 2019, Split, 2019.
[22] Šušnjara A, Verhnjak O, Poljak D, Cvetković M, Ravnik J. "Stochastic-deterministic boundary element modelling of transcranial electric stimulation using a three layer head model". Eng Anal Bound Elem 2021;123(2020):70–83.
[23] Cvetković M, Poljak D, Hausien J. "Analysis of transcranial magnetic stimulation based on the surface integral equation formulation". IEEE Trans Biomed Eng 2015; 62(6):1535–45.
[24] Ackerman MJ. "The Visible Human Project". Proc IEEE 1998;86(3):504–11. March.
[25] U.S. National Library of Medicine. The Visible Human Project, [Online]. Available: https://www.nlm.nih.gov/research/visible/visible_human.html. Accessed September 2019.
[26] S.N. Makarov, G.M. Noetscher and A. Nazarian, Low-Frequency Electromagnetic Modeling for Electrical and Biological Systems Using MATLAB, Hoboken, New Jersey: ohn Wiley & Sons, Inc, 2016.
[27] Electrode Position Nomenclature Committee. "Guideline thirteen: guidelines for standard electrode position nomenclature". J Clin Neurophysio 1994;11:111–3.
[28] ITIS Foundation, "Copyright © 2010–2021 IT'IS Foundation", 2019. [Online]. Available: https://itis.swiss/virtual-population/tissue-properties/database/.
[29] L.C. Wrobel, "The Boundary Element Method", Applications in Thermofluids and Acoustics, vol. 1, 2002.
[30] Xiu D, Hesthaven JS. "High-Order Collocation Methods for Differential Equations with Random Inputs". SIAM J Sci Comput 2005;27(3):1118–39.
[31] Šušnjara A, Dodig H, Cvetković M, Poljak D. "Stochastic dosimetry of a three compartment head model". Eng Anal Bound Elem 2020;117:332–45.
[32] Sobol IM. "Sensitivity Estimates for Nonlinear Mathematical Models". Matematicheskoe Modelirovanie 1990;2:112–8.
[33] Saltelli A, Ratto M, Andres T, Campologno F, Cariboni F, Gatelli D, Saisana M, Tarantola S. Global sensitivity analysis: the primer. West Susex, England: John Wiley & Sons, Ltd; 2008.
[34] Bikson M, Asif R, Datta A. "Computational models of transcranial direct current stimulation". Clin EEG Neurosci 2012;43(3):176–83.